Available online at www.sciencedirect.com
SCIENCE DIRECT®

Journal of the European Ceramic Society 23 (2003) 2361–2366

www.elsevier.com/locate/jeurceramsoc

Silicon nitride/silicon carbide nanocomposite obtained by nitridation of SiC: fabrication and high temperature mechanical properties

M. Poorteman[a,*], P. Descamps[a], F. Cambier[a], M. Plisnier[b], V. Canonne[b], J.C. Descamps[b]

[a]*Belgian Ceramic Research Centre, Avenue Gouverneur Cornez 4, Mons, 7000, Belgium*
[b]*Faculté Polytechnique de Mons, Belgium*

Received 15 August 2002; received in revised form 8 January 2003; accepted 24 January 2003

Abstract

Si_3N_4/SiC nanocomposites have been successfully synthesized according to a novel technique consisting in the nitridation of silicon carbide raw materials followed by their sintering in the presence of appropriate sintering aids. Depending on the kind of additive used, the microstructure of the final nanocomposite can be tailored from elongated silicon nitride matrix grains with silicon carbide nanoparticles dispersed into them, through completely nano-sized composites consisting of equiaxed silicon carbide and silicon nitride grains. Thermomechanical properties are related to those microstructural features and to the secondary phase composition and its subsequent crystallisation.

Keywords: Mechanical properties; Mircostructure-final; Nanocomposites; Nitridation; Si_3N_4–SiC

1. Introduction

Silicon carbide and silicon nitride based ceramics have been extensively studied, particularly because of their excellent mechanical properties at high temperature. Although Si_3N_4 and SiC monolithic ceramics exhibit very attractive properties, the design of Si_3N_4/SiC nanocomposite materials is of particular interest because of their improved high temperature strength and fracture toughness.[1] These materials consist of a submicron-sized Si_3N_4 matrix containing a dispersion of nano-size SiC particles.

Different methods to prepare Si_3N_4/SiC nanocomposites have been reported in the literature such as powder mixing,[2] carbon deposition,[3] polymer pyrolysis.[4] In this paper, we have used a novel fabrication method consisting in the nitridation of silicon carbide powder. The concept is based on the development of an in situ Si_3N_4 matrix/SiC nanoparticle composite by a high-pressure nitridation treatment allowing to obtaining a homogeneous distribution of the reinforcement phase.

An advantage of this method is that it enables to control the Si_3N_4/SiC ratio through the reaction kinetics. Moreover, cheap raw materials and relatively low synthesis temperature can be used.

However, microstructure and mechanical properties strongly depend on the experimental parameters, which have to be controlled carefully.

A necessary condition for the successful fabrication of Si_3N_4/SiC nanocomposites is therefore the knowledge of the thermodynamic stability of the reacting materials. The stability ranges of Si_3N_4 and SiC are shown in Fig. 1.[5] The lower part of the stability range is defined by the decomposition of Si_3N_4 according to:

$$Si_3N_{4(s)} \rightarrow 3Si_{(l)} + 2N_{2(g)}$$

The upper part of the stability range is controlled by the decomposition of SiC according to:

$$3SiC_{(s)} + 2N_{2(g)} \rightarrow Si_3N_{4(s)} + 3C_{(s)}$$

The first silicon nitride phase to be formed by the reaction between SiC and nitrogen at high temperature and high pressure is the α-Si_3N_4 phase, transforming into β-Si_3N_4 phase when nitridation goes on. This $\alpha \rightarrow \beta$

* Corresponding author. Tel.: +32-65-403440; fax: +32-65-348005.
E-mail address: m.poorteman@bcrc.be (M. Poorteman).

0955-2219/03/$ - see front matter © 2003 Elsevier Ltd. All rights reserved.
doi:10.1016/S0955-2219(03)00088-8

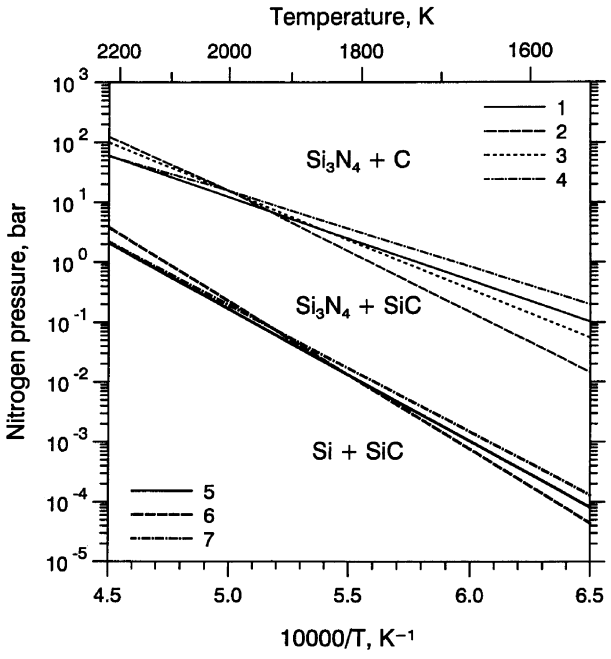

Fig. 1. Thermodynamic stability diagram of Si_3N_4/SiC according to Ref 5.

transformation should preferentially take place during densification to obtain good mechanical properties for the densified ceramic. Therefore, the nitridation reaction should lead to a high amount of α-Si_3N_4 and a low β-Si_3N_4 content. This will enable densification to take place by dissolution of α-Si_3N_4 in an oxide liquid phase and precipitation on pre-existing β-Si_3N_4 grains.

The purpose of the present paper is to study the synthesis of raw mixtures and thermomechanical properties of densified Si_3N_4/SiC nanocomposites.

2. Experimental

For the nitridation experiments, two different compositions were studied. In the *first composition*, we added 1.38 wt.% carbon (KS 6, Lonza) to a pure α-SiC powder (UF10, H.C. Starck, average grain size: ~1 μm) in order to convert surface silica present at carbide grains into silicon nitride, according to:

$$3SiO_{2(s)} + 6C_{(s)} + 2N_{2(g)} \rightarrow Si_3N_{4(s)} + 6CO_{(g)}$$

No sintering aids were added at this stage.

For the *second composition*, we selected a much finer silicon carbide starting powder (UF 45, H.C. Starck, average grain size: ~480 nm) and added 4 wt.% yttria but no additional carbon this time.

The raw materials were mixed in isopropanol in a vibration mill (SWECO) during 16 h, and then dried under air at 60 °C during 24 h.

Dried powder mixtures were compacted by uniaxial followed by cold isostatic pressing (150 MPa) and α-SiC was transformed into silicon nitride by nitridation in a HIP equipment. Nitridation conditions were optimised through changing nitridation temperature (between 1400 and 1650 °C), pressure (between 5 and 200 MPa) and time (between 15 min and 7 h) and by a careful control of reformed crystallographic phases in order to obtain a powder with a high α/β-Si_3N_4 ratio and an α-SiC content between 10 and 20 vol.%

The first composition was vibration milled using alumina balls, which led to a substantial alumina contamination, as observed by XRF. Therefore yttria (4 wt.%) was added during this stage in proportions corresponding to yttria-alumina garnet. In order to avoid alumina contamination, milling was carried out using zirconia media in the case of the second composition.

After a calcination step (700 °C in air during 1 h), the composite powder was finally sintered by hot pressing under 40 MPa at 1750 °C for 1 h in nitrogen atmosphere. Reference monolithic materials using commercial silicon nitride (LC12SX, H.C. Starck) were synthesized using the same processing route for the same final composition except for the nitridation step which was omitted.

The following mechanical properties were assessed on densified samples: fracture toughness (K_{IC}), measured by the SENB technique, using a 3-point bending device; fracture strength (σ_f), determined using a 3 point bending test with a span of 15 mm and a crosshead displacement of 0.1 mm/min; microhardness measured at room temperature by Vickers indentation with an applied load of 10 N; creep tests, performed with the same 3-point bending equipment, at 1200 °C, while maintaining a constant load of 80 MPa, under nitrogen atmosphere. Microstructures of the materials were observed by transmission electron microscopy (TEM).

Crystallographic phases present in dense materials were determined by XRD analysis and the composition was calculated semi-quantitatively from complete XRD spectra using an iterative computing method taking corundum as a standard.[6]

3. Results and discussion

3.1. Optimisation of nitridation conditions

During nitridation a transformation of α-SiC into α-Si_3N_4 was always observed first, followed by a further conversion into β-Si_3N_4.

Optimum conditions for the first composition, using a micron-sized powder (UF10), were obtained at 1600 °C, during 7 h, under a 50 MPa nitrogen pressure.

Using finer nano-sized powder (UF45) in composition 2, the nitridation temperature could be reduced to

1400 °C, keeping time and pressure as in the first procedure. The crystallographic composition of the powder mixture obtained for each composition is shown in Table 1.

XRD analysis revealed a strong dependence of crystallographic composition on nitridation route. With the finest SiC having higher oxygen content, using yttria in the starting composition and adding no graphite, a high quantity of Si_2ON_2 phase is formed. Moreover, the kinetics of the α-Si_3N_4 to β-Si_3N_4 conversion seem to be accelerated with respect to the α-SiC to α-Si_3N_4 transformation, which is very likely explained by the presence of a liquid phase during the nitridation process, favouring the α-Si_3N_4 dissolution and reprecipitation of β-Si_3N_4. Consequently, the composite powder mixtures show quite different crystallographic compositions.

3.2. Material synthesis and characterisation

3.2.1. First composition (nitridation conditions: 1600 °C–7 h, 50 MPa N_2)

After hot pressing, a dense composite with a crystallographic composition represented in Table 1 is obtained.

A complete α-Si_3N_4→β-Si_3N_4 transformation took place and some secondary phases, Si_2ON_2 and $Y_2Si_3O_3N_4$ (belonging to the Y_2O_3–SiO_2–Si_3N_4 phase diagram[7]), are formed.

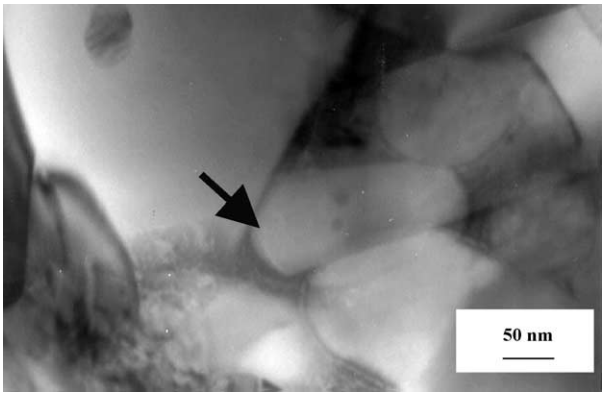

Fig. 2. Microstructure obtained by TEM observation of the Si_3N_4/SiC nanocomposite (composition 1). The arrow shows a glassy pocket at a triple point.

TEM observation, however, reveals the presence of a considerable quantity of glassy phase as can be seen in Fig. 2 where we observed glassy pockets and round-shaped silicon nitride grains. Generally, the microstructure is characterised by needle-like and equiaxed Si_3N_4 grains (Fig. 3). SiC grains are spherical and are located both at grain boundaries and inside Si_3N_4 grains (Figs. 4 and 5).

The average microhardness of the nanocomposite is 1526±25 and only 1397±47 for the monolithic material. The hardness increase can be attributed to the higher

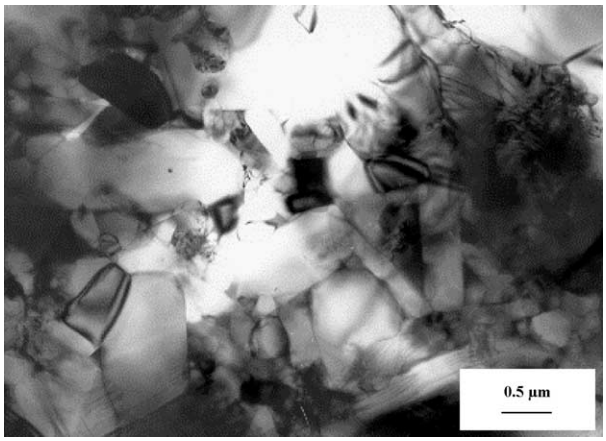

Fig. 3. Global TEM observation of the Si_3N_4/SiC nanocomposite (composition 1).

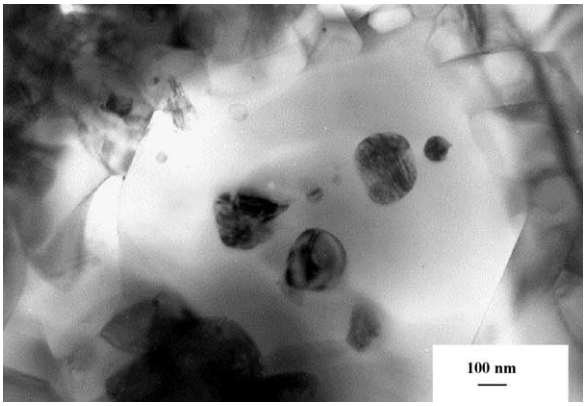

Fig. 4. Intragranular SiC present in the Si_3N_4/SiC nanocomposite (composition 1).

Table 1
Crystallographic phases (wt.%) calculated from XRD spectra of nanocomposite powders obtained by nitridation of several starting compositions and after hot pressing

State	Composition	α-Si_3N_4	β-Si_3N_4	α-SiC	Si_2ON_2	$Y_2Si_3O_3N_4$	$Y_2Si_2O_7$
Nitrided	1	85	2	13	0	–	–
	2	41	16	18	25	–	–
Hot pressed	1	0	73	14	5	8	–
	2	0	50	17	25.5	–	7.5

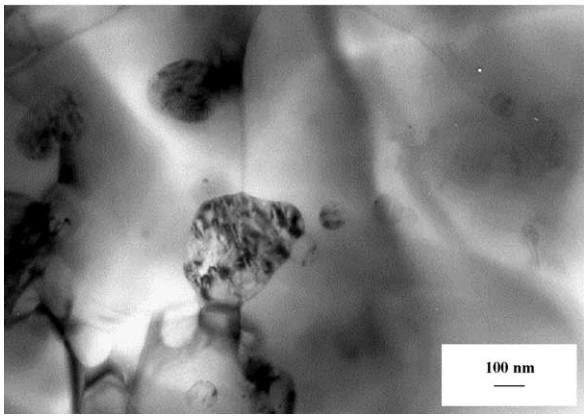

Fig. 5. Grain boundary pinning by intergranular SiC present in the Si_3N_4/SiC nanocomposite (composition 1).

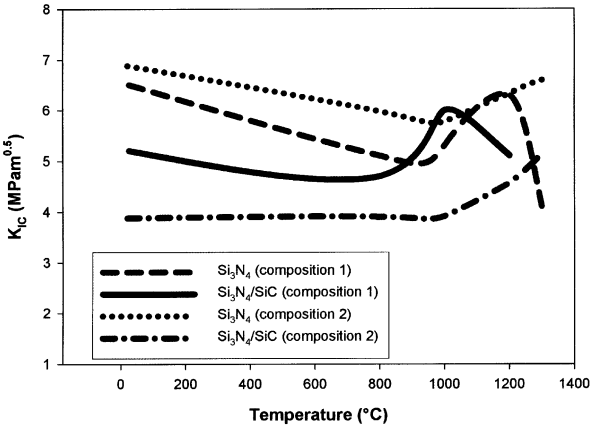

Fig. 6. Toughness variation of different nanocomposites and monolithic materials with temperature.

hardness of SiC (about 2000) compared with the monolithic matrix, and follows the law of mixture.

Room temperature toughness of the nanocomposite is slightly lower than that of the matrix (Fig. 6). As mentioned before, the microstructure of the matrix of the nanocomposite is mixed and consists of elongated as well as equiaxed β-Si_3N_4 grains, whereas it is generally known that the microstructure of hot pressed silicon nitride consists exclusively of crosslinked β-Si_3N_4 favouring a toughness increase by a crack deflection mechanism.

At high temperature fracture toughness, first, decreases, up to around 800 °C and, then, goes through a maximum value at about 1000–1100 °C before decreasing again at higher temperatures. This can be explained by plastic deformation between 800 and 1000 °C. In this temperature range, the residual glassy phase transforms into a liquid phase with high viscosity. The increase of toughness can then be explained by the lowering of the crack tip stress intensity in the plastic zone ahead of the crack, by energy dissipation through relaxation occurring in the grain boundary phase. At higher temperature, above *Tg* the glass transition temperature, the glassy phase becomes more liquid and grain boundary sliding predominates plastic relaxation and leads to matrix decohesion with a decrease of mechanical properties as a consequence.

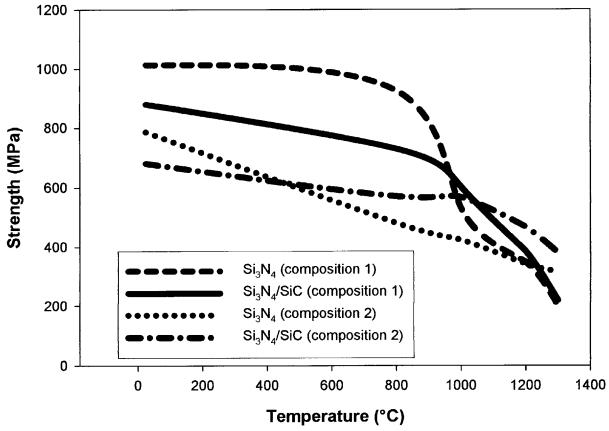

Fig. 7. Strength variation of different nanocomposites and monolithic materials with temperature.

Room temperature strength of the nanocomposite is lower than that of the monolithic material (Fig. 7). This can be explained by its lower room temperature toughness. Strength also decreases with temperature. However, the strength decrease of the nanocomposite is lower compared with the monolithic material, which might be attributed to grain boundary pinning by intergranular SiC particles impeding grain boundary sliding.

For the same reason we can explain the higher creep resistance of the nanocomposite at 1200 °C (Creep rate: $\dot{\varepsilon}(Si_3N_4) = 5.0\ 10^{-8}\ s^{-1}$, whereas $\dot{\varepsilon}(Si_3N_4/SiC) = 3.0\ 10^{-8}\ s^{-1}$).

At this stage, the feasibility to fabricate Si_3N_4/SiC nancomposites by the proposed approach has been proven. However, no substantial increase in high temperature mechanical properties is obtained working with this first composition. Therefore, materials were fabricated with a composition intended to favour the high temperature mechanical properties using more refractory sintering aids (pure yttria).

3.2.2. Second composition (nitridation conditions: 1400 °C–7 h, 50 MPa N_2)

After hot pressing a dense composite with a crystallographic composition shown in Table 1 is obtained.

Again, compared with the nitrided powder, α-Si_3N_4 completely transformed into β-Si_3N_4. However, the amount of Si_2ON_2 did not change. Compared with the first composition, β-Si_3N_4 content is somewhat lower (50 instead of 72%) and a higher amount of Si_2ON_2 is obtained (25.5 instead of 5%). SiC content is comparable, but Y_2SiO_7 crystallises instead of $Y_2Si_3O_3N_4$.

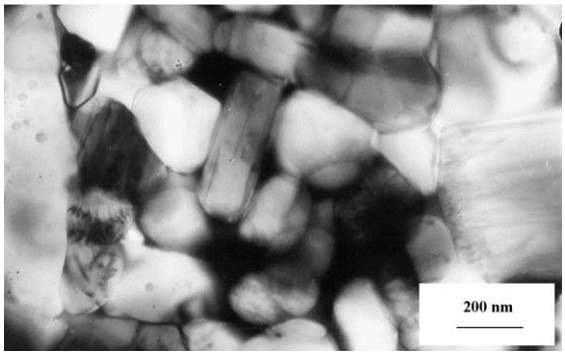

Fig. 8. Global TEM observation of the Si_3N_4/SiC nanocomposite (composition 2).

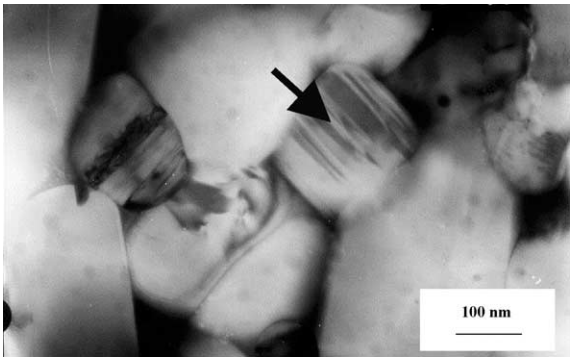

Fig. 9. Arrow showing SiC present in the Si_3N_4/SiC nanocomposite (composition 2).

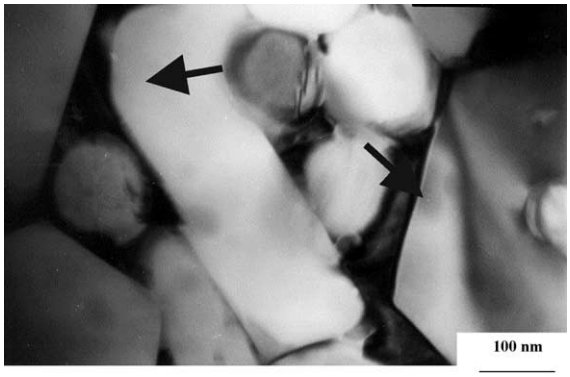

Fig. 10. TEM observation of recrystallised intergranular phase (arrows) in the Si_3N_4/SiC nanocomposite (composition 2).

TEM observation showed the microstructure to be completely different: Si_3N_4 grains are mostly equiaxed and very small sized (<500 nm), whereas spherical SiC grains are mostly intergranular with sizes around 200 nm (Figs. 8 and 9).

Although some glassy phase was present at triple points and grain boundaries, a high degree of intergranular crystalline phase was observed (Fig. 10). Consequently, an improved refractoriness can be expected for this material.

Microhardness of the nanocomposite is largely improved compared to that of the monolithic material: H_v (Si_3N_4) $= 1515 \pm 18$ whereas H_v (Si_3N_4/SiC) $= 1770 \pm 20$.

This increase in hardness can only be partially attributed to the presence of harder SiC particles, as the law of mixture cannot completely explain the hardness increase. Therefore, we also have to consider the crystallisation of the residual glassy phase and the very fine microstructure which can also give rise to a hardness increase.

Toughness variation as a function of temperature is given in Fig. 6 and appears to be different compared to the behaviour found in the case of procedure one. Indeed, the room temperature toughness of the nanocomposite is much lower than that of the monolithic material due to its very fine and completely equiaxed microstructure. This results in less crack/microstructure interaction (such as crack deviation) leading to a lower toughness. Up to 1000 °C, toughness progressively decreases in the case of the monolithic material but not for the nanocomposite. Starting from 1000 °C, there is a continuous increase of K_{IC} up to the maximum tested temperature (1300 °C). In this case also, liquid phase formation starting from the glass transition temperature (1000 °C) induces the formation of a plastic zone ahead of the crack tip allowing energy dissipation to occur. However, contrary to the previous material (composition 1), the viscosity of the glassy phase remains very high as a function of temperature, probably due to the absence of Al^{+++} ions. Therefore, the relaxation phenomenon in the plastic zone remains efficient at much higher temperatures and the toughness continues to increase. Strength variation as a function of temperature is shown in Fig. 7.

The lower strength of the nanocomposite compared to that of the reference silicon nitride at room temperature can be explained by its lower toughness ($K_{IC} = 3.9$ MPa$\sqrt{m}$ instead of 6.9 MPa$\sqrt{m}$ for silicon nitride) which can in turn be related to the finer microstructure of the composite. Indeed, as suggested above this will very likely limit reinforcement by crack deviation. However, at the same time, the very fine microstructure of the nanocomposite also leads to a smaller flaw size and, therefore, the room temperature strength is only slightly lower compared to that of the reference matrix.

At elevated temperature, i.e. starting from 800 °C, the room temperature strength of the nanocomposite is maintained and becomes significantly higher compared to the monolithic material. This difference can no longer be explained in terms of a SiC grain boundary pinning mechanism as these particles have the same size as the Si_3N_4 grains. This time, we have to consider that below the glass transition temperature (1000 °C), both matrix toughness and strength decrease with temperature in the case of the monolithic material whereas in the case of the nanocomposite both remain almost constant. This difference in temperature dependence of

mechanical properties might have several reasons: the high crystallisation degree of the nanocomposite allowing maintaining a high material stiffness as a function of temperature; differences in glassy phase composition and again crystallisation degree could lead to a higher subcritical crack growth resistance. To confirm these hypotheses, further experiments have to be carried out, such as the determination of the grain boundary composition for instance by HRTEM, quantification of the crystallisation degree and determination of the fatigue parameter n below the glass transition temperature.

4. Conclusions

Si_3N_4/SiC nanocomposite powders can be successfully synthesised by nitridation of α-SiC powder under high N_2 pressure. The final composition of this powder can be tailored through controll of reaction kinetics (time, pressure and temperature).

The synthesis temperature can be significantly reduced by selecting finer starting powders. Microstructure, secondary phase composition and subsequent crystallisation as well as thermomechanical properties are correlated with the sintering aid system. In the case of the Al_2O_3/Y_2O_3 system (YAG composition), higher room temperature mechanical properties are obtained due to the needle like morphology of Si_3N_4 grains leading to a tough material. However, residual glassy phase leads to the formation of a liquid phase at high temperature and therefore to a lack of refractoriness.

In the case of the Y_2O_3 system, the microstructure of the hot pressed material is completely different and consists of equiaxed SiC and Si_3N_4 grains. Therefore, toughness and consequently strength are lower. However, due to the high crystallisation degree the room temperature strength of the nanocomposite is maintained up to 1000 °C and only slightly decreases above this temperature ($\sigma_{f\ 1300\ °C} = 380$ MPa).

References

1. Lange, F. F., Effect of microstructure on strength of Si_3N_4/SiC composite systems. *J. Am. Ceram. Soc.*, 1973, **56**, 445.
2. Pezzotti, G. and Sakai, M., Effect of a silicon carbide nanodispersion on the mechanical properties of silicon nitride. *J. Am. Ceram. Soc.*, 1994, **77**(11), 3039–3041.
3. Niihara, K., Hirano, T. and Izaki, K., High temperature creep/deformation of Si_3N_4/SiC nanocomposites. In *Ceramic Transactions, Vol. 42, Silicon-Based Structural Ceramics*, ed. B. W. Sheldon. American Ceramic Soc., Westerville, OH, 1994, pp. 207–219.
4. Riedel, R., Seker, M. and Becker, G., Sintering of amorphous polymer—derived Si, N, and C containing composite powders. *J. Eur. Ceram. Soc.*, 1989, **5**, 113–122.
5. Herrmann, M., Schuber, C., Rendtel, A. and Hubner, H., Silicon nitride/silicon carbide nanocomposite materials: fabrication and mechanical properties at room temperature. *J. Am. Ceram. Soc.*, 1989, **81**(5), 1095–1108.
6. Deletter, M., Leriche, A. and Cambier, F., A linear model for both qualitative and quantitative X-ray analysis. *Sil. Ind.*, 1998, **57**, 3–8.
7. Tien, T. Y., Petzow, G., Gauckler, L. J. and Weiss, J., Phase equilibrium studie in Si_3N_4/metal oxides systems. In *Progress in Nitrogen Ceramics*, ed. F. L. Riley. Martinus Nijhoff Publishers, Boston/The Hague/Dordrecht/Lancaster, 1983, pp. 89–99.